HIGH PERFORMANCE MICROGYROS FOR SPACE APPLICATIONS

Tony K. Tang, Roman C. Gutierrez, Ken Hayworth, Chris Evans,
Judith A. Podosek, Allan Hui, Damien Rodger, Kirill Shcheglov

Jet Propulsion Laboratory
MicroDevices Laboratory, California Institute of Technology
4800 Oak Grove, Pasadena, CA 91109-8099

ABSTRACT

This paper reports on the development of a high performance silicon bulk micromachined vibratory gyroscope designed for microspacecraft applications. This silicon vibratory microgyroscope consists of a four-leaf clover silicon structure with a central post suspended by four thin silicon cantilevers. This device is electrostatically actuated at one of its mechanical modes, and input rotation is detected by monitoring the Coriolis induced motions of the leaves capacitively. The bias stability of this microgyroscope is typically < 10 deg/hr with angle random walk of < 0.1 deg/√hr, and scale factor nonlinearity of <1%. This new vibratory microgyroscope offers potential advantages of long operational life, high performance, extremely compact size, low power operation, and low cost.

INTRODUCTION

Present inertial measurement systems that use conventional gyroscope technologies are exceedingly costly, massive, and consume too much power for microspacecraft applications. Micromachined vibratory gyroscopes[1-5] are promising candidates to replace conventional gyroscopes for navigation, guidance, and attitude control applications in future microspacecraft missions.

In this paper, we report on recent developments of a silicon bulk micromachined vibratory gyroscope. This silicon vibratory microgyroscope is fabricated using simple, precise, and low-cost bulk silicon machining technology. This unique symmetric, high quality (Q) factor resonator design results in a highly sensitive device.

This high performance microgyroscope will be integrated into a micro Inertial Reference System (μIRS) chip consisting of three orthogonal silicon micromachined vibratory gyroscopes and accelerometers. This μIRS chip will be used for attitude and maneuver control, and stabilization and pointing of instruments such as cameras, antenna, detectors, and solar panels. The μIRS chip can also supplement other external inertial reference systems[6] such as the Global Positioning System (GPS), sun sensor, or star tracker by "filling in the gaps" during times the direct use of these systems is not possible.

DESCRIPTION

The general mechanical structure of this silicon microgyroscope consists of a four leaf clover suspended by four thin wires with a post rigidly attached to the center in the direction perpendicular to the plane of the clover leaves (Figure 1). The silicon cloverleaf structure with the post is bonded to a silicon base plate patterned with gold electrodes. The cloverleaves provide large surface area for electrostatic drive and sensing. The four suspensions provide mechanical support and restoring force for the harmonic motion of the whole structure.

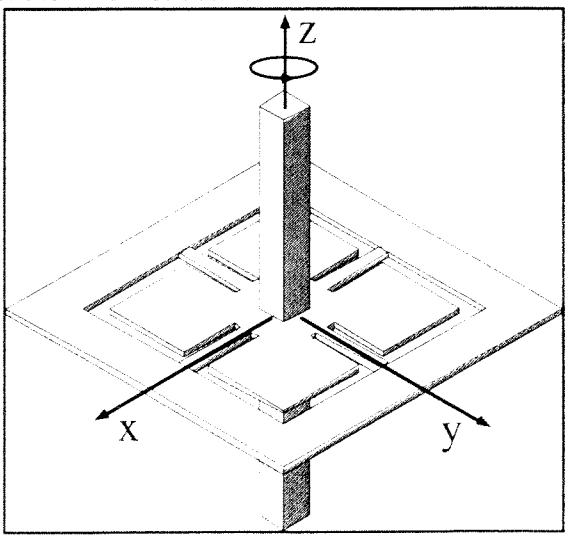

Figure 1. Schematic drawing of the microgyro structure.

The post provides a large Coriolis force coupling between the orthogonal modes when the gyroscope rotates about the post axis. The mechanical resonant frequencies of the microgyroscope is designed to be in 2500 to 3000 Hz range. The first three mechanical modes are 1) up/down mode in which all the leaves move along the z-axis simultaneously, 2) rocking mode about the y-axis, and 3) rocking mode about the x-axis. The two rocking modes of the cloverleaf structure are symmetrical in the x-y plane and are inherently degenerate with the same identical resonant frequency. The cloverleaf structure is electrostatically driven to oscillate at the "drive" mode, rocking about one of the in-plane axes (i.e. y-axis). Since the post is rigidly attached to the cloverleaf structure, the post moves along the x-direction. Under rotation, Coriolis acceleration induces energy transfer from the "drive" mode to the orthogonal "sense" mode causing the post to rock about the y-axis (in addition to its initial drive motion about the x-axis). The motion of the post is translated back into the rocking motion of the cloverleaves. The post provides a large Coriolis coupling which transfers energy between the two orthogonal rocking modes. The highest rotation sensitivity is obtained when the drive and sense modes have the same resonant frequency. Very stringent fabrication and assembly requirements are necessary to achieve this "matched" condition. When this "matched" condition is achieved, the response to the Coriolis acceleration is then amplified by the Q factor of the resonance resulting in improved sensor performance and reduced drive voltage.

FABRICATION

The cloverleaf microgyroscope design consists of three major components: the silicon cloverleaf structure, the silicon baseplate, and the vertical silicon post. The starting material for the cloverleaf structure is <100> silicon double side polished wafers with two epilayers grown on top. The buried epilayer is 4 microns thick doped with Boron ($10^{20}/cm^3$) and counter-doped with 2% Ge for stress relief. The top silicon epilayer is 26 microns thick doped with Phosphorous. The baseplate starting material is <100> silicon double side polished wafers that is 3mm thick.

The fabrication procedure for the cloverleaf structure begins with the deposition of a thin layer (1000Å) of thermal SiO_2 onto the silicon wafer. This SiO_2 layer is patterned with the clover leaf pattern and used as a mask for the wet chemical etching of the 26 microns silicon epilayer. This etch is self-terminated at the p+ etch-stop layer.

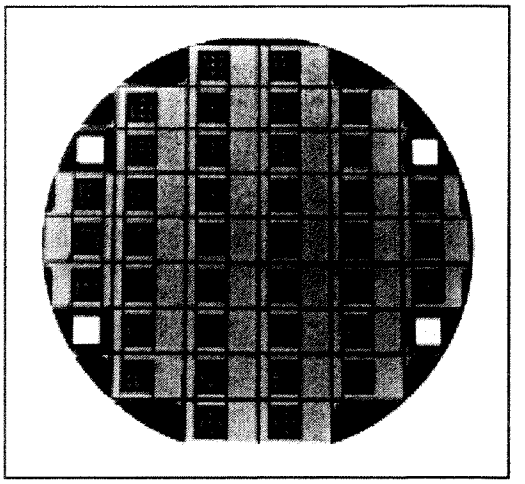

Figure 2. Cloverleaf structures on a 4-inches silicon wafer.

After the wet chemical etch, the first thin SiO_2 layer is removed and a 5000Å thick SiO_2 is grown on the entire wafer. The SiO_2 on the backside of the wafer is then patterned and etched. Layers of chromium, platinum and gold are then e-beam evaporated onto the cloverleaf structure and patterned. The whole wafer is then etched in ethylene diamine pyrocatechol (EDP) to remove the silicon substrate. Again this wet etch self terminate at the p+ etch-stop layer (Figure 2). Next, the wafer is reactive ion etched with SF_6 and O_2 to remove the p+ stop-etch layer. Finally, the remaining SiO_2 layer is removed using a CF_4/O_2 plasma.

The fabrication process of the silicon baseplate also begins with the deposition of a thin layer (1000Å) of thermal SiO_2 onto the silicon wafer. The SiO_2 layer is then patterned and etched with EDP to the depth of 8 microns. This depth will be the gap distance separating the cloverleaf structure and the baseplate electrodes. After the first EDP etch, a thick thermal silicon dioxide and layer is grown onto the whole wafer. The topside oxide layer is patterned and etched to provide electrical contact to the substrate. Metallization

consisting of CrPtAu is then e-beam evaporated onto the topside of the silicon wafer and patterned to form the electrodes. The backside oxide layer is also patterned and etched. Then entire wafer is etched in EDP to open a hole through the substrate to accommodate the post.

The cloverleaf structure and the baseplate wafers are bonded together using a low temperature thermocompression bonding method. In this process, gold metallization on the clover leaf structure and the baseplate are heated to 300-600°C in vacuum. Then pressure is applied to the entire structure for several hours to bond the components together. During this bonding process, gold diffusion is enhanced by the application of heat and pressure, and results in a metal bond. This bond is very strong; the silicon structures usually shatter before the bond fails. The total bond line is < 4000 Å thick and uniform (Figure 3).

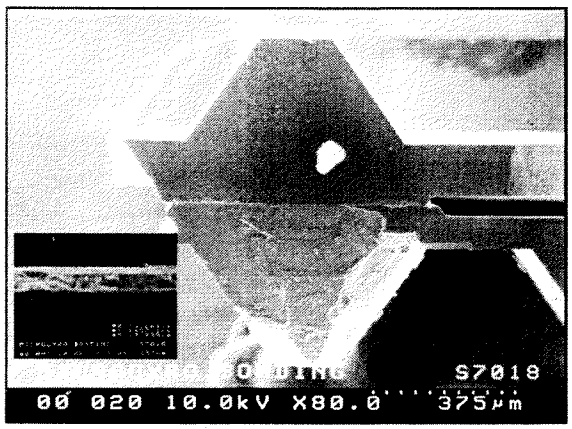

Figure 3. Bonded components using low temperature gold thermocompression bonding. The inserted SEM picture shows the gold bond line between two silicon wafers.

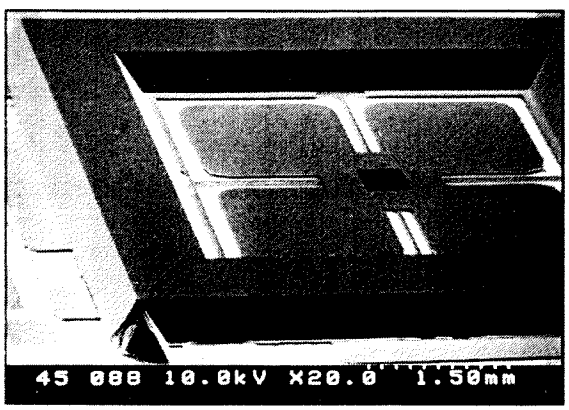

Figure 4. SEM picture of bonded cloverleaf structure with silicon baseplate before the assembly of the central post.

The bonded devices (Figure 4) are first tested for resonant frequencies and mode shapes. After these initial tests, a silicon post is epoxied into the hole on the silicon resonator. The dimensions of the silicon clover-leaf structure is 7 mm x 7 mm, the dimensions of each clover leaf is 2 mm x 2 mm, and the post is 500 microns square and 5 mm in length. The silicon base plate is 1 cm x 1 cm and is approximately 3 mm thick.

CONTROL AND READOUT ELECTRONICS

The actuation, or drive, circuit is realized by designing an oscillator (H(s)) around the microgyroscope which locks onto the drive resonance mode as shown in Figure 5. The purpose of summing the signals from both sense plates is to remove the differential signal between them and hence the response of the sense resonance is obtained from the feedback loop. The sense circuit, on the other hand, subtracts the signals from both sense plates in order to remove the common-mode drive signal. A lock-in amplifier is used to detect a differential signal induced due to rotation.

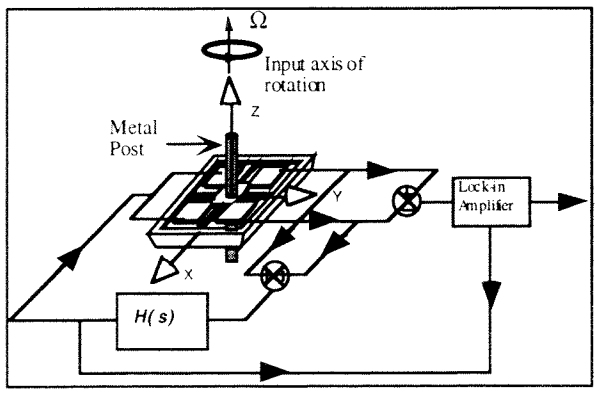

Figure 5. Block diagram of the microgyro control electronics.

MEASUREMENT

The mechanical characteristics of the microgyroscopes are first identified in a custom test station consisting of a vacuum chamber with electrical probes to electrically excite the microgyroscope, and a Polytech OFV 501 laser vibrometer (Doppler velocimeter) to accurately measure mechanical motion. This system is used to measure

the resonance frequencies, Q-factors, mode shapes, hysteresis, snap-down voltage, symmetry (by exciting different electrodes), operational voltage, and survivability (by driving it with a very large amplitude signal) of the microgyroscope. The rotation testing of the microgyroscope uses a Triotech S347B rate table with a resolution of 0.01 degrees per second to rotate a microgyroscope inside a vacuum chamber, and a computer to record the output of the gyroscope as a function of rotation rate.

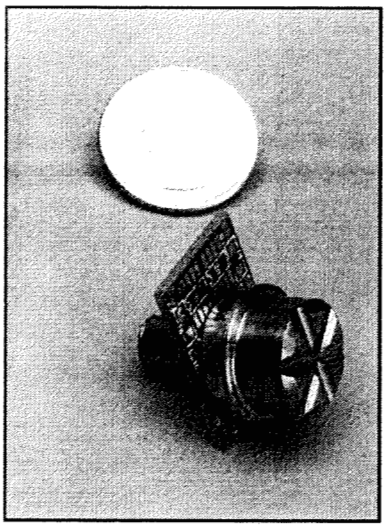

Figure 6. Packaged microgyro with control electronics.

The silicon microgyroscopes tested to date have mechanical resonant frequencies ~3000 Hz, with a frequency split of <0.1%. The Q-factor of the drive and sense modes is typically 1,000 to 10,000. Both resonant modes are rocking modes with nodal lines along the spring directions. The separation between the resonant frequencies is primarily due to thickness variations between the silicon suspensions and stress due to the bonding of the post to the clover leaf structure. Due to the close proximity of the "drive" and "sense" resonant frequencies, the response of these device are amplified by Q. The microgyroscope is vacuum packaged into a stainless steel package (Figure 6)

The response of the microgyroscope to rotation rates is taken between -2 deg/sec and +2 deg/sec at room temperature. The driving voltage of the microgyroscope is approximately 100 mV peak to peak. Three consecutive tests are done to check for hysterisis and scale factor stability. Typical scale factor stability is 0.1% under ambient conditions with no hysteresis. The Green chart, which plots the two-sampled standard deviation (square root of the Allan variance) as a function of the integration time, is used to characterize the noise. Obtained values for angle random walk noise and bias stability are consistently < 0.1 deg/√hr and < 5 deg/hr, respectively.

INTEGRATED GYROS

To further improve the performance of the cloverleaf microgyroscope, the mechanical structure of the device has been modified to include an integrated post. One half of the post is fabricated from the silicon wafer that the cloverleaf is made from, and the other half of the post is made from the silicon baseplate wafer (Figure 7). This design simplifies the fabrication process and eliminates the post assembly procedures. These devices have been fabricated and is undergoing mechanical and rotation testings. Initial results showed that these devices have less than <0.1% in frequency split (Figure 8).

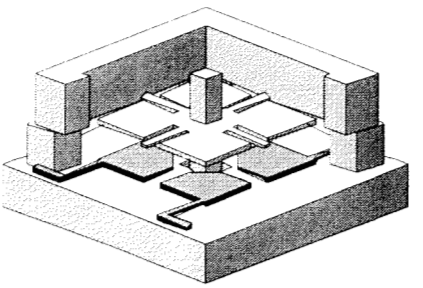

Figure 7. Schematic drawing of the integrated gyro with integrated silicon post.

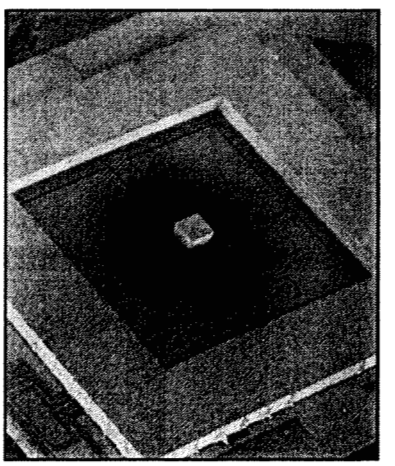

Figure 8. SEM picture of the integrated gyro with integrated post.

The μIRS chip is a six degree of freedom inertial measurement unit. It consists of three accelerometers, in-plane rate gyros, and a z-axis (out-of-plane) rate gyro. These inertial sensors are fabricated on a single chip and bonded to a control electronics chip to form the μIRS chip (Figure 9). The separation of the inertial sensors and electronics allows the use of optimized structure (epilayer, dielectric layers, metallization) and fabrication process to provide the best device performance.

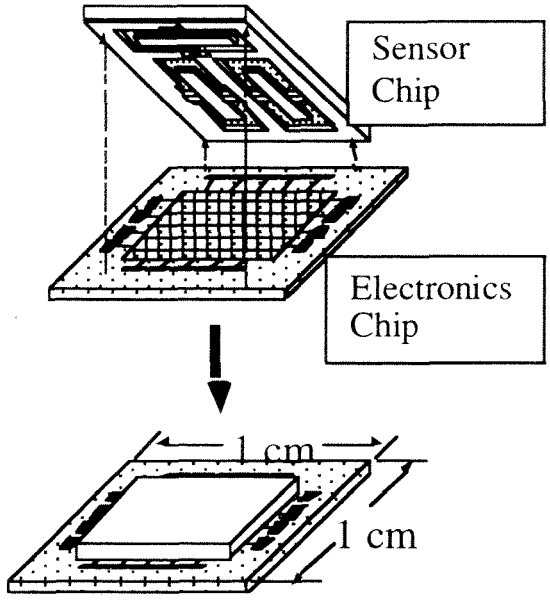

Figure 7. Schematic drawing of the μIRS chip consists of separated sensor and electronics chips.

CONCLUSION

This paper report on recent experimental results on a new generation of silicon cloverleaf microgyroscope designed for micro inertial reference system on a single chip for microspacecraft applications. These new microgyroscopes have consistently demonstrated a bias stability of < 5 deg/hr, and a rate random walk of < 0.1 deg/√hr with open-loop electronics and no temperature compensation. The cloverleaf vibratory microgyroscope offers potential advantages of long operational life, high performance, extremely compact size, low power operation, and low cost for applications in inertial navigation and attitude control of microspacecraft. Continual improvement and optimization of the cloverleaf microgyroscope will result in performance of less than 1deg/hr bias stability in the near future.

ACKNOWLEDGMENTS

The work described in this paper was performed by the Center for Space Microelectronics Technology, Jet Propulsion Laboratory, California Institute of Technology, under contract with the National Aeronautics and Space Administration.

REFERENCE

1 M. W. Putty, and K. Najafi, Tech. Digest, Solid-State Sensor & Actuator Workshop, Hilton Head Isl., SC, pp. 213-220, June 1994.

2 J.Bernstein, S.Cho, A.T.King, A.Kourepenis, P.Maciel, M.Weinberg, Digest, IEEE/ASME MEMS Workshop, Ft. Lauderdale, Fl., pp. 143-148, February 1993.

3 P.Ljung, T.Juneau, and A.Pisano, Proceedings of the ASME Dynamic Systems and Control Division, DSC-Vol. 57-2, 1995 IMECE/ASME, pp. 957-962.

4 T.Tang, R.Gutierrez, J.Wilcox, C.Stell, V. Vorperian, R.Calvet, W.Li, I.Charkaborty, R.Bartman, W.Kaiser, Tech Digest, Solid-State Sensor & Actuator Workshop, Hilton Head Isl., S.C. pp.288-293, June 1996.

5 T.Tang, R.Gutierrez, C. Stell, V.Vorperian, G.Arakaki, J.Rice, W.Li, I.Chakraborty, K.Shcheglov, J.Wilcox, W.Kaiser, Digest, IEEE/ASME MEMS Workshop, Nagoyo Castle, Japan, January 1997.

6 G.Sevaston, L.Craymer, & W.Brecken-ridge, 19th AAS Guidance & Control Conference, Breckenridge, CO, AAS 96-16, pp. 1-20. Feb. 7-11,1996